Numerical Investigation Of Rigid Microparticles Dynamics: Aggregation And Clogging Phenomena In Microfluidics By Discrete Element Method (DEM) And CFD Coupling

K. Shahzad, W. Van Aeken, V. Kazemi Kamyab, M. Mottaghi and S. Kuhn

KU Leuven, Department of Chemical Engineering, Leuven, Belgium, khurram.shahzad@kuleuven.be

ABSTRACT

We develop numerical solvers to study and understand the phenomena of aggregation and clogging of rigid microparticles suspended in a Newtonian fluid passing through a straight microchannel. Initially, we use a time-dependent one-way coupling Discrete Element Method (DEM) technique to simulate the movement and effect of adhesion on microparticles in 2D & 3D. The aggregation and deposition behavior of particle-particle and particle-wall contacts are investigated by varying the Reynolds number and adhesion parameter in a non-periodic channel. The contact mechanics between particle-particle interactions was implemented by using the Johnson-Kendall-Roberts (JKR) theory of adhesion. In addition, we also employ a two-way coupling (CFDEM coupling) approach. One and two-way coupling techniques will provide us an insight on hydrodynamic effects by predicting wall deposition and clogging behavior in microfluidic devices. Results in terms of microstructures, aggregates percentage and spatial and temporal evaluation of aggregates in 2D & 3D will be compared, respectively.

Keywords: Aggregation, Adhesion, Clogging, Rigid suspensions, Microfluidics, Discrete Element Method (DEM), CFD-DEM simulation, OpenFOAM

1 Introduction

Microfluidics has achieved a positive response in the industrial sector in the last two decades, i.e., due to its minute size plus control over all the chemical and physical properties at various flow rates (Re 1-10) and with less safety issues [1]. However, utility and lifetime are some of the common challenges present with those devices to sustain a flow without disruption. Particularly, microparticle wall deposition which initiates dendritic structures which end up clogging the whole microchannel or microfluidic device [2, 3]. Therefore, extensive academic and industrial studies have been carried out to inspect the clogging behavior happening in microfluidic devices for suspension flows under numerous situations.

Generally, particulate flow experience different forces frequently, i.e., surface forces with nearby channel walls, inertial forces, buoyant weight and drag force [4, 5, 6]. Aggregation is initiated due to weak (van der Waals) attraction forces which leads to larger size aggregates and this phenomenon is called agglomeration. However, another phenomenon is present in suspension flow, where large size aggregates break down in smaller aggregates which is called fragmentation [7]. But any unbalance between the agglomeration and fragmentation process can lead the system towards clogging of the channel.

To understand the physical mechanism of clogging is extremely complex, with the simplest description that the microchannel cross-section is constricted due to particle deposition, which, together with an increase in the agglomerate size, leads to clogging. Another possibility is arch formation, where particles position themselves in an arch formation in such a way that high shear forces hold particles together and along the channel walls thus jam the whole arch [8, 9, 10].

In the current study, we used a Discrete Element Method (DEM) to simulate the aggregation, agglomeration and fragmentation of spherical rigid particles suspended in a Newtonian fluid flowing through a straight microchannel. As compared to previous literature, we adopt a non-periodic channel that is initially filled by the Newtonian fluid without any particles. Later, rigid microparticles are injected in the microchannel through the inlet section at a fixed injection rate so the overall volume fraction is maintained at a constant number. Thus, it is quite helpful for us to understand the aggregation/fragmentation phenomena during the initial stage of injecting particles in the microchannel. We investigate the aggregate formation and breakage based on two parameters, the Reynolds number and adhesion force strength. 2D & 3D one-way coupling simulations are compared in order to check the effects of the dimensionality on aggregate formation and clogging phenomena, plus 3D two-way couplings simulations are also compared, respectively.

2 Mathematical model

We study a suspension flow of spherical particles in a microfluidic channel with 2D and 3D (cylindrical channel). Here, we assume that the particles are transported only by the fluid, plus the particles do not modify the carrying fluid flow field, and this whole method is called one-way coupling approach [11]. The overall particles dynamic is simulated through the Discrete Element Method (DEM), where particle translational and angular velocities are solved [12, 13, 14].

$$m\frac{d\boldsymbol{v}}{dt} = \boldsymbol{F}_{\mathrm{D}} + \boldsymbol{F}_{\mathrm{A}} \tag{1}$$

$$I\frac{d\boldsymbol{\Omega}}{dt} = \boldsymbol{M}_{\mathrm{D}} + \boldsymbol{M}_{\mathrm{A}} \tag{2}$$

where, m is the particle mass, I is the momentum of inertia, $\boldsymbol{v}$ is the particle translation velocity and $\boldsymbol{\Omega}$ is the particle angular velocity. We neglect the motions of sliding, rolling and twisting of a particle on another. The forces considered here are only the fluid drag force $\boldsymbol{F}_{\mathrm{D}}$, and the sum $\boldsymbol{F}_{\mathrm{A}}$ of the van der Waals adhesive force and the elastic collision force. Based on our assumptions, Eq. (1) is decoupled from Eq. (2), i.e. it is not required to compute the particle angular velocity to calculate the translation velocity. Therefore, we use only Eq. (1) throughout our simulations. In addition, we assumed a 'freeze' boundary condition for particles. So, when a single particle touches a channel wall, it will permanently attached at the wall during the whole simulation.

In these studies, we implement a JKR model [17], to simulate the agglomeration and aggregate formation in suspension flow [11, 15, 16].

The fluid force experienced by each particle present in laminar flow is given by the drag force $\boldsymbol{F}_{\mathrm{D}}$:

$$\boldsymbol{F}_{\mathrm{D}} = -3\pi d\mu(\boldsymbol{v} - \boldsymbol{u}) \tag{3}$$

where, $\boldsymbol{u}$ is the fluid velocity and μ is the fluid viscosity. The adhesion and collision force $\boldsymbol{F}_{\mathrm{A}}$ shown in Eq. (1) is modeled based on our assumption, by neglecting the overall effect of the sliding of each particle over another particle [15]. Hence, the interparticle adhesion/collision force contains only the normal force:

$$\boldsymbol{F}_{\mathrm{A}} = F_{\mathrm{n}}\boldsymbol{n} \tag{4}$$

where, F_{n} is the normal force magnitude and $\boldsymbol{n}$ is the unit vector which connects the centers of two particles:

$$\boldsymbol{n} = \frac{\boldsymbol{x}_j - \boldsymbol{x}_i}{|\boldsymbol{x}_j - \boldsymbol{x}_i|} \tag{5}$$

where, $\boldsymbol{x}_i$ and $\boldsymbol{x}_j$ are the position vectors of two particles i and j.

The normal elastic force magnitude F_n can be calculated as a function of the contact region radius a [17, 18]:

$$\frac{F_n}{F_{\mathrm{C}}} = 4\left(\frac{a}{a_0}\right)^3 - 4\left(\frac{a}{a_0}\right)^{3/2} \tag{6}$$

where, F_{C} is the critical force:

$$F_{\mathrm{C}} = 3\pi\gamma R \tag{7}$$

in which, γ is the van der Waals surface potential energy and R represents the effective radius of the colliding particles. The contact region radius a is linked to the particle normal overlap δ_{N}, through the following equation:

$$\frac{\delta_{\mathrm{N}}}{\delta_{\mathrm{C}}} = 6^{1/3}\left[2\left(\frac{a}{a_0}\right)^2 - \frac{4}{3}\left(\frac{a}{a_0}\right)^{1/2}\right] \tag{8}$$

with the critical overlap

$$\delta_{\mathrm{C}} = \frac{a_0^2}{2(6)^{1/3}R} \tag{9}$$

In above Eqs. (6), (8) and (9), a_0 is the equilibrium radius:

$$a_0 = \left(\frac{9\pi\gamma R^2}{E}\right)^{1/3} \tag{10}$$

For each particle Eq. (1) is integrated over time. Therefore, to boost the computations, we generate a look up table for Eqs. (6)-(8) before the simulations. In addition, we use a neighbor-list algorithm so that only particles at a certain distance from each other are included in the collision/adhesion force evaluation step. Furthermore, the whole channel length is distributed into vertical blocks ($d + \delta_{\mathrm{C}}$) in a manner that the colloidal/adhesion forces are calculated only for particles residing in three consecutive blocks.

2.1 Parameter definition

Table 1: Parameters used in the simulations. The last columns indicate the final time for the 2D and cylindrical (3D) channel cases.

Cases	d_p	Re	ϕ	λ	$t_{2D}, t_{3D}(sec)$
A.1	10	5.25	15	$2.93 \cdot 10^8$	5
A.2	10	5.25	150	$2.93 \cdot 10^8$	5
A.3	10	5.25	1500	$2.93 \cdot 10^8$	5
A.4	10	5.25	15000	$2.93 \cdot 10^8$	5
B.1	10	7.0	15	$1.65 \cdot 10^8$	5
B.2	10	7.0	150	$1.65 \cdot 10^8$	5
B.3	10	7.0	1500	$1.65 \cdot 10^8$	5
B.4	10	7.0	15000	$1.65 \cdot 10^8$	5
C.1	10	10.5	15	$7.35 \cdot 10^7$	5
C.2	10	10.5	150	$7.35 \cdot 10^7$	5
C.3	10	10.5	1500	$7.35 \cdot 10^7$	5
C.4	10	10.5	15000	$7.35 \cdot 10^7$	5

Our system contains particles of $d = 10$ µm in diameter with a microchannel length of $L = 2$ mm. In 2D, the channel width (gap) is set to $H = 0.25$ mm, and in 3D the channel radius is set to $R_{\mathrm{cyl}} = 0.125$ mm. Initially, there are no particles present in the fluid. The

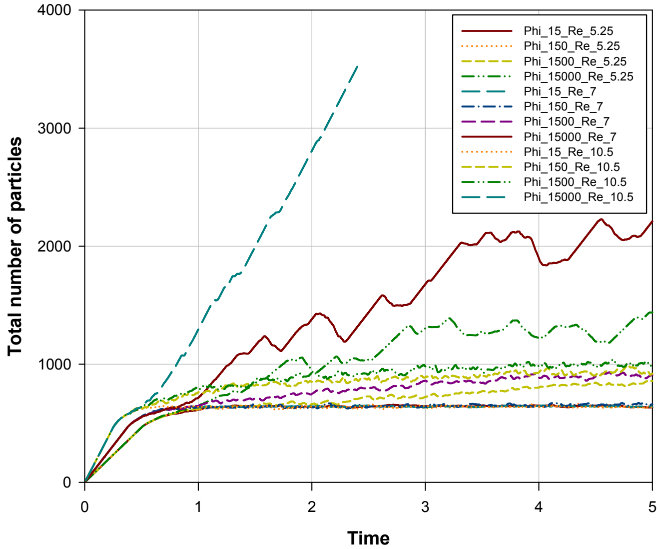

Figure 1: Total number of particles present inside the channel

particles are injected at a fixed frequency near the inlet section with a velocity, which is set equal to the local fluid velocity. We used two different volume fraction values of $\phi_V = 0.1$ for the 2D case and $\phi_V = 0.05$ for the 3D case. To replicate the realistic approach in our system we used non-periodic boundary conditions, so when any particle crosses the outlet section, it is immediately removed from the simulation. The values of the parameters are selected for rigid particles with the particle density $\rho_p = 1000$ kg/m^3, the fluid density $\rho_f = 1000$ kg/m^3, the fluid viscosity $\mu = 10^{-3}$ Pa·s, and the elastic modulus of the particles $E = 1$ GPa. The average fluid velocity is taken to be $u_{avg} = 2.91, 3.889, 5.83$ mm/s. The values of the Reynolds number, the adhesion parameter and the elasticity parameter used in the simulations are showed in Table 1. Furthermore, a very small time step is required to assure steadiness and accuracy of the numerical computations to calculate the collision and adhesion force between particles.

3 Results and Discussion

In the current studies, dynamics of particle-particle, particle-aggregate, aggregate-aggregate and aggregate-wall interactions are investigated by changing the Reynolds number and adhesion parameter. Figures 2 display instantaneous images of the particle distribution over the entire microchannel (2D case) for $Re = 5.25$, 7.0, 10.5, respectively. In this figure, twelve images are shown corresponding to different values of the adhesion parameter increasing from 15 to 15000 from top to bottom. All the screen shots are taken at the final time step. To study the rate of aggregate creation, we define three sections

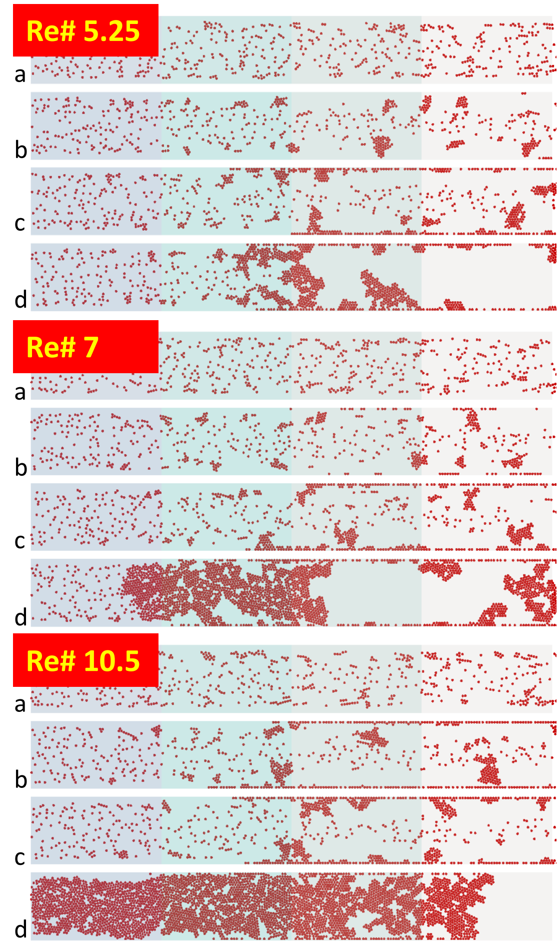

Figure 2: Snapshots of the particle distribution through a channel for all 2D cases

that divide the whole microchannel in four parts. The channel inlet is at $x = 0.0$ and the outlet is at $x = 8.0$ (where x represents the dimensionless coordinate in flow direction), the first section point is at $x = 2.0$, the second section point is at $x = 4.0$, the third section point is at $x = 6.0$, and the last point is at the outlet $x = 8.0$.

It is observed, that higher adhesion parameter values increase the formation of large aggregates at a fixed Reynolds number (Fig. 2)(d) for all Re#. However, a lower adhesion parameter value shows no major influence on aggregate formation, as only small aggregates made up of 2–3 particles are generated, but an increase in the adhesion parameter value results in the formation of large size aggregates, specifically in the near wall region. As the number of wall attachment increases, these aggregates are later detached from the channel walls due to the high shear forces exerted by the incoming fluid. When the CFDEM coupling technique is used by fixing the adhesion parameter and at a high Reynolds number of $Re = 10.5$, both the formation of large aggregates and wall attachment is observed.

4 Conclusions

The results indicate that aggregates start to be generated near the walls, where the highest velocity gradients are present. The particle-aggregate and aggregate-aggregate interactions may produce new contacts with the walls. We impose a freeze boundary condition, so when the first layer of particles is developed on the walls, then there is either the possibility that particles/aggregates may attach to that layer or are detached from the layer due to the large fluid induced force. If this fluid induced force is not large enough then a growing structure arises at the microchannel walls, which eventually leads to the clog/blockage of the whole microchannel. The increase in the total number of particles inside the microchannel and the investigation of the size of the aggregates show that the creation of larger aggregates is promoted by large Reynolds numbers and high adhesive forces. However, 3D results show that the size of the aggregates are much larger than in the 2D case, whereas the 2D case exhibits a high aggregate formation rate with very few particles.

Furthermore, we used a two–way coupling approach to investigate the dynamical effect of particles/aggregates on the fluid phase in 3D. There we observe that a large number of wall attachments are formed at a large Reynolds number of $Re = 10.5$ compared to the one–way coupled case.

REFERENCES

[1] Tabeling, Patrick. "Introduction to microfluidics", New York: Oxford University Press, 2007.

[2] Hartman, Ryan L. "Overcoming the challenges of solid bridging and constriction during Pd-Catalyzed CN bond formation in microreactors." Organic Process Research and Development 14.6 (2010): 1347-1357.

[3] Flowers, Brian S., and Ryan L. Hartman. "Particle Handling Techniques in Microchemical Processes."Challenges 3.2 (2012): 194-211

[4] Sharma, M. M., and Y. C. Yortsos. "Fines migration in porous media." AIChE Journal 33.10 (1987): 1654-1662.

[5] Herzig, J. P., D. LECLERK, and P. LeGoff. "Flow of suspensions through porous media." Chemische Technik. Vol. 22. No. 3. Karl Heine Str 27b, 04229 Leipzig, Germany: Deutscher Verlag Fur Grundstoffindustrie, 1970.

[6] McDowellBoyer, Laura M., James R. Hunt, and Nicholas Sitar. "Particle transport through porous media." Water Resources Research 22.13 (1986): 1901-1921.

[7] Henry, Christophe, et al. "A new stochastic approach for the simulation of agglomeration between colloidal particles." Langmuir 29.45 (2013): 13694-13707.

[8] Goldsztein, Guillermo H., and Juan C. Santamarina. "Suspension extraction through an opening before clogging." Applied physics letters 85.19 (2004): 4535-4537.

[9] Sharp, K. V., and R. J. Adrian. "On flow-blocking particle structures in microtubes." Microfluidics and Nanofluidics 1.4 (2005): 376-380.

[10] Mustin, Benjamin, and Boris Stoeber. "Deposition of particles from polydisperse suspensions in microfluidic systems." Microfluidics and nanofluidics 9.4-5 (2010): 905-913.

[11] Marshall, J. S. "Particle aggregation and capture by walls in a particulate aerosol channel flow." Journal of Aerosol Science 38.3 (2007): 333-351.

[12] Landry, James W., et al. "Confined granular packings: structure, stress, and forces." Physical review E 67.4 (2003): 041303.

[13] Cundall, Peter A., and Otto DL Strack. "A discrete numerical model for granular assemblies." geotechnique 29.1 (1979): 47-65.

[14] You, C. F., et al. "Motion of micro-particles in channel flow." Atmospheric Environment 38.11 (2004): 1559-1565.

[15] Shahzad, Khurram, et al. "Numerical investigation of hard-gel microparticle suspension dynamics in microfluidic channels: Aggregation/fragmentation phenomena, and incipient clogging." Chemical Engineering Journal 303 (2016): 202-216.

[16] Marshall, J. S. "Discrete-element modeling of particulate aerosol flows." Journal of Computational Physics 228.5 (2009): 1541-1561.

[17] Johnson, K. L., K. Kendall, and A. D. Roberts. "Surface energy and the contact of elastic solids." Proceedings of the Royal Society of London A: Mathematical, Physical and Engineering Sciences. Vol. 324. No. 1558. The Royal Society, 1971.

[18] Chokshi, Arati, A. G. G. M. Tielens, and D. Hollenbach. "Dust coagulation." The Astrophysical Journal 407 (1993): 806-819.